Feasibility study of medium power helicon thruster

D.Pavarin[1] M.Manente[2], Y.Guçlua[3], D.Curreli[3] , C.Bettanini[2], M.Zaccariotto[2],
CISAS university of Padua 35131 Padova

M. Walker[4], D.Palmer[5]
High-Power Electric Propulsion Laboratory, Georgia Institute of Technology, Atlanta, GA, 30332, USA

J. Carlsson[6]
Tech-X corporation, Boulder CO USA

C. Bramanti[7]
Advanced Concept Team ESA ESTEC Noordwijk - The Netherlands

And
E.Lorenzini[8]
Department of mechanical Engineering University of Padua

A medium power (1.5 kW) plasma thruster based on helicon source has been recently considered as a possible candidate for primary space propulsion. A high-density plasma is produced by the use of a radio frequency transmitting antenna, producing helicon waves to ionise a neutral gas (e.g. argon, krypton, xenon, helium or hydrogen) flowing through a tube and confined by a magnetic field. The plasma is then accelerated through a potential drop created by a rapidly expanding magnetic field giving a sudden reduction in electron density (and hence plasma potential) very close to the open end of the source tube and then expanded through a "magnetic nozzle" into vacuum. Numerical studies has been conducted by CISAS in order to investigate the physics connected with the potential drop. The analysis has been conducted through a combination of 1-D and 2-D code numerical code. A specific 1-D code named PPDL has been developed for this purpose. Main feature of the code are: hybrid Boltzmann electron/drift-kinetic ion, inclusion of dominant 2-D effects, high computational efficiency thorough implicit non linear Boltzmann solver. The 2-D XOOPIC is open source code available from Berkeley University. Limitations of XOOPIC are no floating boundary conditions implemented on the electrostatic solver and long computational time. The combined approach resulted very useful since the 1-D code has been used to screen many different experimental conditions and to identify the right boundary conditions. The 2-D code has been then used to refine 1-D results. The two models, combined with a global model, specifically developed to simulate the plasma reaction inside the plasma source, have been finally run through genetic algorithms to identify an optimal thrusters configuration in the 1500 W power regimes. In addition the thruster has been thermally and mechanically sized.

[1] Researcher, Department of Mechanical Engineering University of Padova Via Venezia 1 35131 Padova
[2] Post-doc fellow CISAS University of Padua Via Venezia 1535131 Padova Italy
[3] PhD student CISAS University of Padova 35131Via Venezia 15 Padova Italy
[4] Associate professor High-Power Electric Propulsion Laboratory, Georgia Institute of Technology, Atlanta, GA, 30332, USA
[5] PhD student High-Power Electric Propulsion Laboratory, Georgia Institute of Technology, Atlanta, GA, 30332, USA
[6] Senior researcher, Tech-X corporation, 5621 Arapahoe Ave Suite A, Boulder, CO 80303
[7] ESA technical officer, Advanced Concept Team ESTEC - DG-PI, Keplerlaan 1 - 2201 AZ Noordwijk - The Netherlands
[8] Full professor Department of Mechanical Engineering University of Padova Via Venezia 1 35131 Padova

Nomenclature

A = cross surface of the cell revolution
A_{Exh} =geometrical exhaust area
BSCCO = Bismuth Strontium Calcium Copper Oxide
Cp =coefficient
c_s =coefficient
E_{THi} =Threshold energy for i-th reaction
e =electron charge
Isp = specific impulse
K_i =reaction rate for i-th specie
K_B = Boltzmann constant
L_{Exh} =ion lost at the exhaust
M =particle mass
m_{ion} =ion mass
n =plasma density
n_e =electron density
n_i =density of i-th specie
n_j =density of the specie involved in the *i*-th reaction
Pabs =deposited power
P_{EXH} =power loss accociated with the electron and ion flux at the exhaust
P_i =power lost in the *i*-th reaction
P_w =power lost at the exhaust
r =radius of magnetic lines tube
r_i =radius of the detachment cell
r_p =plasma radius
S/C =spacecraft
T =particle temperature
Te =electron temperature
U_B = ion Bohm velocity
V_a = average axial velocity inside the detachment cell
V_e =plasma volume
Z =position
Γ_{EXH} =flux loss term due to the particle flow through the exhaust for the *i*-th specie
Γ^l_i = flux loss term due to plasma process for the *i*-th specie
Γ^s_i =flux source term due to plasma process for the *i*-th specie
Γ_{Wi} =flux loss term due to particle recombination at wall for the *i*-th specie
σ =cross section

I. Helicon Thruster Numerical Models

The modeling approach proposed here is based on three different numerical models: 1) a global numerical model of the plasma source, 2) a 1-D PIC code of the entire system , 3) a 2-D PIC code of the entire system. The global model is used to simulate the plasma source behavior, it provides the source ionization rate, plasma density and electron temperature to the other two codes. A 1-D code named PPDL was specifically developed for this purpose. It is a hybrid code with Boltzmann electrons and drift-kinetic ions, inclusion of dominant 2-D effects and high computational efficiency through implicit nonlinear Boltzmann solver. The 2-D code used was XOOPIC, freely available from University of California at Berkeley. With XOOPIC it was necessary to perform fully electrostatic simulations with kinetic electrons, resulting in long computational times in order to analyze detachment features. A combined approach proved very useful where the 1-D code was used to rapidly screen many different experimental conditions and to identify the right boundary condition. The 2-D code was then used to refine the 1-D results.

A. Plasma source numerical model

A global model to describe the plasma source has been developed. This approach is similar to other global models previously developed[5-10] . The plasma balance equations for particles and energy have been written for describing a uniform distributed plasma inside of a region confined by a magnetic field.

Many studies have been carried out to understand the interactions between plasma and neutrals, including the effect of neutral losses to ionization[5-8,26,27]and neutral heating[18-19]. Several models take into account the neutrals density inserting a source term and a sink term into the neutrals balance equation[5-9,12-17]. These terms are related respectively to the feeding flow from the reservoir and the flow to the vacuum pump. In other models the plasma neutral interactions are not considered and no equations are written to follow the neutrals density behavior[10,11] . Due to the specific gas-dynamic configuration of the device, the neutral interaction with plasma has been considered in this work by coupling a 0-dimensional gas-dynamic model of the entire system, with a global plasma model of the source.

This model provides an estimate for the pop-off feeding-valve operation, efficiency of neutral pumping by the vacuum pump, efficiency of a gas trap in the source to increase the ionization efficiency. The interactions that are taken into account in the model are:

- neutral density reduction due to ionization;
- neutral dissociation (molecular specie-atom species);
- zero dimensional gas dynamic analysis behavior in the plasma source and in the vacuum chamber;
- wall recombination and volume recombination in the main vacuum chamber.

Plasma is generated in the source chamber. A preliminary investigation shows that in specific magnetic field configurations or in a specific operation mode (helicon mode), the plasma could be confined inside of a volume smaller than the source chamber volume[1] .

Plasma has been considered confined in a cylindrical volume V_e defined by a radius, plasma radius r_p, and having the same length than the source chamber, L. Inside this volume different species are considered for every gas. The model follows the density of all of these species. Plasma flows and diffuses also through the external surfaces of the volume V_e. These surfaces will be named in different way to highlight the different process involved. The back axial surface is the surface in front of the feeding orifice, plasma in this zone is electrostatically confined and the mass loss is calculated using Godyac and Maximov[25] solution of diffusion equation. Plasma diffuses also through the radial surface, but in this zone the magnetic field generated by the solenoid coil improves the confinement. The particle loss in this area has been calculated using again the Godyac and Maximov solution modified by Cheetham[10] to take into account the magnetic field contribution to the confinement. The axial surface toward the vacuum chamber is named exhaust surface. Plasma flows in this zone with a speed that is a fraction of the ion sound velocity. The speed depends strongly on the shape of the plasma potential in this area. Being this calculation beyond the purpose of this model, a parameter has been introduced into the numerical analysis named cs. Therefore the exhaust velocity is the ion sound velocity multiplied by the cs coefficient that has been considered as a free parameter. Particles that diffuse through the lateral surface and through the back axial surface are neutralized.

The plasma equations are coupled with neutral equations since in the source chamber the neutrals density is not constant but free to change in relation to the neutral flow, the dissociation processes and the plasma-neutral interaction. The reactions involving ionized species and electrons are found in literature[23,28]. The particle balance equations for the ionized particles and electrons are written in a particle flux form, (particles/seconds m^3). The general form for the balance equations of charged particles is:

$$\frac{dn_i}{dt} = \Gamma_i^s - \Gamma_i^l - \Gamma_{Wi} - \Gamma_{EXH-i} \tag{1}$$

where Γ_i^s is for the i-specie the source term due to plasma processes, Γ_i^L is the loss term due to plasma processes, Γ_{Wi} is for the i-specie the loss term due to particle recombination at the wall (the particle diffuses through the wall sheath before reaching the wall), Γ_{EXH} is the loss term due to the particle flow through the exhaust. The reaction rates were obtained averaging the cross section for the specific reaction over a Maxwellian distribution[28] :

$$K_i = \left(\frac{m}{2\pi kT}\right)^{3/2} \int_0^\infty \sigma(v) v \exp\left(-\frac{mv^2}{2kT}\right) 4\pi v^2 dv \tag{2}$$

where T is the electron temperature in eV and m is the particle mass and σ the cross section. Wall losses are calculated as in (Ref.5-7,17). Ions lost at the exhaust are calculated as:

$$L_{EXH} = n_i \cdot u_B \cdot A_{EXH} \cdot cp$$
$$u_B = \sqrt{\frac{kT_e}{m_i}} \tag{3}$$

u_B term is the ion Bohm's velocity and A_{EXH} is the geometrical exhaust area.
Another parameter affects the exhaust flow. At the exit of the plasma discharge section the magnetic field increases and then decreases. This peak acts as a magnetic mirror that reflects part of the plasma flow. Therefore the net flow is given by the difference between the incident flow and the reflected flow. The reflected flow depends on the configuration of the magnetic field and on the plasma parameters. To calculate the electron temperature, the power balance equation has been written as follows (units: W/m^3)

$$\frac{P_{ABS}}{Ve} = \frac{d}{dt}\left(\frac{3}{2} \cdot e \cdot n_e \cdot T_e\right) + \sum P_i + P_W + P_{EXH} \tag{4}$$

where P_{ABS} is the deposited power into the plasma that is assumed to be known. e is the electron charge, T_e is the electron temperature, V_e again the plasma volume. P_i terms are the power lost in the i-reaction. The general formula is:

$$P_i = K_i \times E_{TH\text{-}i} \times n_e \times n_j \tag{5}$$

where K_i is the rate constant for the specific reaction, $E_{TH\text{-}i}$ the threshold energy for the i-reaction[23], n_e the electron density, n_j the density of the specie involved in the i-reaction. P_W is the power lost at the wall due to the electron-ions flow. P_{EXH} is the power loss associated with the electron and the ion flux at the exhaust, assuming that the escaping velocity is the ion-Bohm velocity. Experimental results[33] indicate the presence of a hot tail in the electron population in hydrogen and helium discharge. This distribution has been modelled summing two maxwellian distributions: one with the temperature of the bulk of the plasma and one with the temperature of the hot tail.

B. 1-D PIC Numerical model

The PPDL is a modified version of an existing 1-D PIC named PadPIC, a Particle in Cell[35,43] plasma simulator. The main features of PPDL are:

- Drift-kinetic ions, where the magnetic moment is assumed to be an adiabatic invariant. The drift-kinetic equation of motion includes the ΔB force from the expanding magnetic field
- The expansion of the magnetic field is considered
- Boltzmann electrons, assuming Maxwellian distribution and inertialess.
- Floating boundary conditions.
- Plasma generation is simulated through a source term.

The advantage of Boltzmann electrons is that electron time scale (plasma and gyro periods) do not have to be resolved, but on the other hand it requires a non-linear Poisson solver to determine the electrostatic potential. With the hybrid Boltzmann electron/drift-kinetic ion approach, the time step is only limited by ion period, which is two orders of magnitude larger than electron plasma period and ion gyro period, which can become very short in a strong magnetic field.. Thus, PPDL is very fast and efficient and still capable of simulating the relevant physics. To better fit the experimental set-up, the presence of magnetic field is simulated by the analytic solution of a field generated by one or more solenoids. The gradient of the magnetic field is also calculated analytically and used for adding the ∇B velocity to the drift-kinetic ions. The dilution of the charge density due to the expanding magnetic field has also been incorporated into the non linear Poisson solver.
A plasma of radius r_0, density n_0, and temperature T_e created in a uniform field B_0 and then injected into a region of expanding field lines has been considered. In the model has been also added the hypotesis that, considering the plasma frozen to the field lines, the field B(z) and the density n(z) in the expansion region are related to the plasma radius as:

$$\frac{n}{n_0} = \frac{B}{B_0} = \left(\frac{r_0}{r}\right)^2 \tag{6}$$

where r(z) is the radius of magnetic lines at position z.

C. 2-D OOPIC Numerical model

As previously mentioned, the code used for the 2-D simulation is the OOPIC (or XOOPIC, which has a GUI), open-source from Berkeley University. OOPIC (Object-Oriented Particle-In-Cell) is a 2D-3V relativistic electromagnetic PIC code. The object-oriented paradigm provides the opportunity for advanced PIC modelling, increased flexibility, extensibility and efficiency[34]. OOPIC includes 2-dimensional orthogonal grid: cartesian (x,y) or cylindrically symmetric (r,z) and moving window, together with electrostatic and electromagnetic fields, and relativistic particles. The boundaries can be determined at runtime and include many models of emitters, collectors, wave boundary conditions and equipotentials. Because the dependence on the azimuthal angle is not expected to be relevant for DL experiments, we can use a 2D r-z cylindrical PIC simulation. The code can handle an arbitrary number of species, particles, and boundaries. It also includes Monte Carlo collision (MCC) algorithms for modelling collisions of charged particles with a variety of neutral background gasses. Figure 1 presents the geometry configuration used for the simulations.

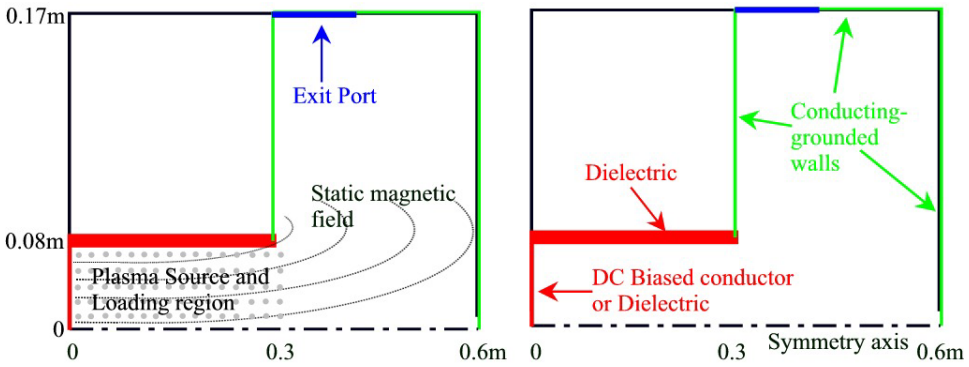

Figure 1 Geometry configuration used on Xoopic simulation

A detailed model of the helicon source is not our intention, the reproduction of its heating process can be avoided by imposing ad hoc electron and ions families, emerging from the source tube. This is a versatile approach because it is possible to change the parameters, simulating plasma expansion in different conditions. The resolution of the particles motion is done under electrostatic assumption. Few particles are immediately loaded into the source region, to represent the high energy electrons produced during the breakdown and to start without an empty region, while the most are created during the simulation. The plasma production is represented by the OOPIC PlasmaSource object. The particles are created at a given rate in a rectangular area and with Maxwellian velocity distribution and a changeable density distribution. The plasma production density is defined in order to model the typical helicon source behavior: maximum density near r=0 and after the tube half (Figure 2). The static magnetic field has been calculated by solving the equations for circular filamentary coils in 2-D. The two solenoids have been located around the source tube at r=12-13 cm, axial positions of 1 and 20 cm and length of 8 cm

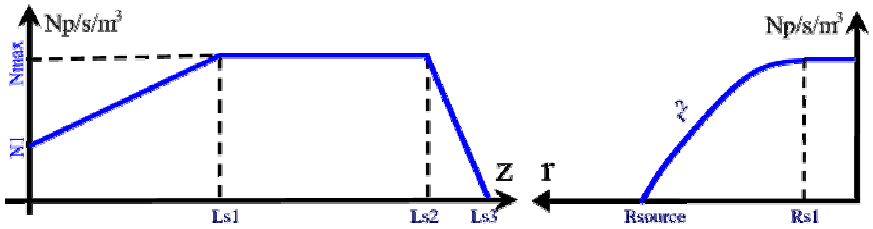

Figure 2 Plasma rate density distribution: Ls3=Lsource=30cm, Rs1=1.5cm and N1=Nmax/3

II. Performance Evaluation: Thrust and Isp

The thrust has been calculated with OOPIC for four different detachment lines. Those lines have been selected considering the axial positions from which the direction of the ions' velocity starts to be constant. We supposed that the distance from the helicon tube exit, where the detachment takes place, grows with the axial position. It is considered greater than 20 cm at the tube axis and almost constant but more than 60 cm for r>30 cm. There we applied the formula $T=\sum m N V_a^2 A$, iterated for every r_i along the supposed detachment line, where *m* is the ion mass, *N* is the density of ions inside the detachment cell at radius r_i, V_a is the average axial velocity inside the detachment cell and *A* is the cross surface of the cell revolution along φ $A=\pi[(r_i+dr)^2-r_i^2]$. Therefore for all the cells that follow the selected line we have evaluated the ions' density, which is a default output of OOPIC, and the average ions' axial velocity. The result is a thrust between 1e-9 and 7e-9 N; it has been obtained comparing three simulations made with Te=8 eV, 70 V dc bised left wall and diffusion chambers 1 m long with different electrical properties. The performed simulations reached a density, inside the source tube, around $5\ 10^{13}$ m^{-3}, the source rate has been set between 10^{18} and $3\ 10^{18}$ $m^{-3}\ s^{-1}$.
The specific impulse (Is) can be evaluated through the formula $Is=(\sum N\ V_a)/(\sum N\ g)$, iterated again along the supposed detachment line and where *g* is the gravitational acceleration.

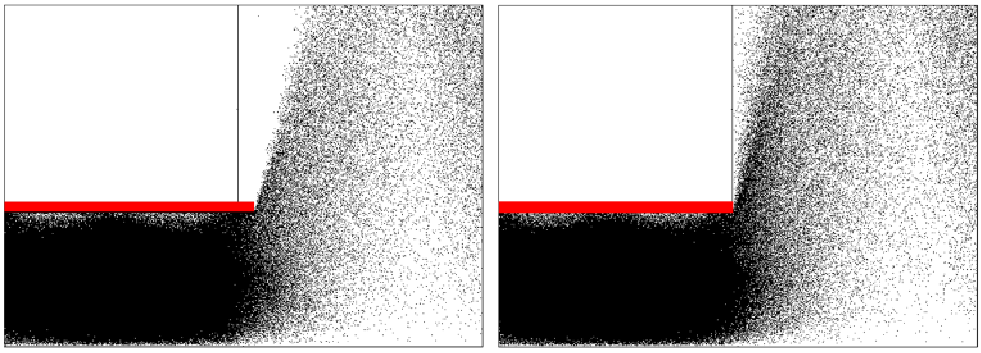

Figure 3 Ion (on the right) and electron (on the left) trajectory at the exhaust.

III. Thruster Design

The thruster has been designed through the combination of the results coming from the numerical simulations and a genetic optimization algorithm
The models described above have been combined with a lumped structural model providing, depending on the selected thruster configuration (i.e mass flow, magnetic field , power etc.), the total volume and mass.
A genetic optimization algorithm has been then used to identify the best thruster configuration as a trade off among performances, weight, and volume.
The global model was initially used in combination with the structural model to identify the most promising configurations, than all of them has been analyzed with the 1-D PIC model in order to identify three best configuration which has been finally investigated with the 2-D PIC code in order to evaluate thrust and Specific impulse.
The power was fixed at 1500 W, the magnetic field was fixed at 1000 Gauss in order to allow very compact thruster, keeping the Larmor radius compatible with the thruster size. The genetic optimization algorithm identified as best trade-off among high Isp and Thrust the following set-up:

Source diameter	25 mm
Source length	70 mm
Mass flow rate	0,05 kg/sm^3

In the following diagrams it is reported the variation of electron density, electron temperature, specific impulse and thrust varying the feeding mass flow rate. As expected increasing the mass flow rate electron density increase but electron temperature reduces and thus ISP.

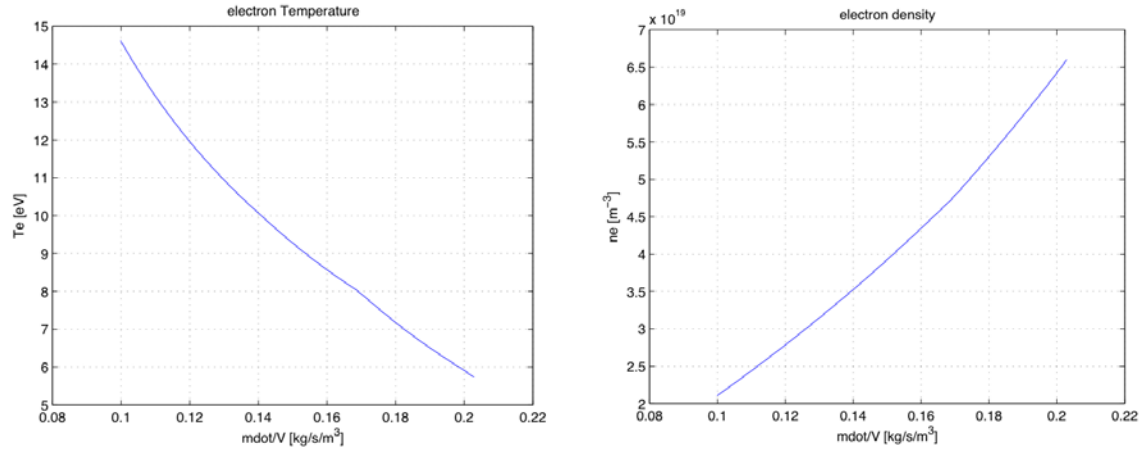

Figure 4 Electron temperature, electron density and neutral density versus mass flow rate normalized on the source volume.

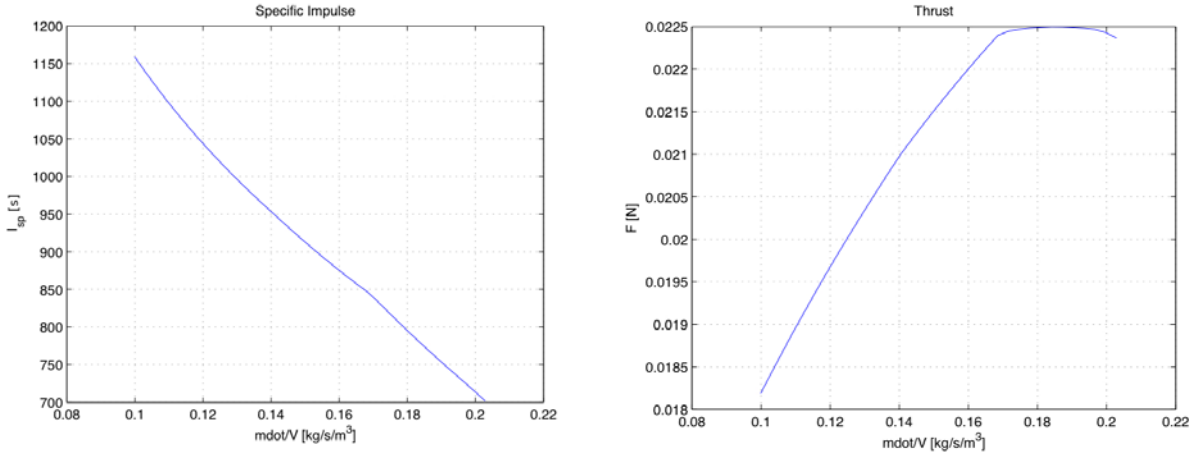

Figure 5 Specific impulse and thrust versus mass flow rate normalized on the source volume..

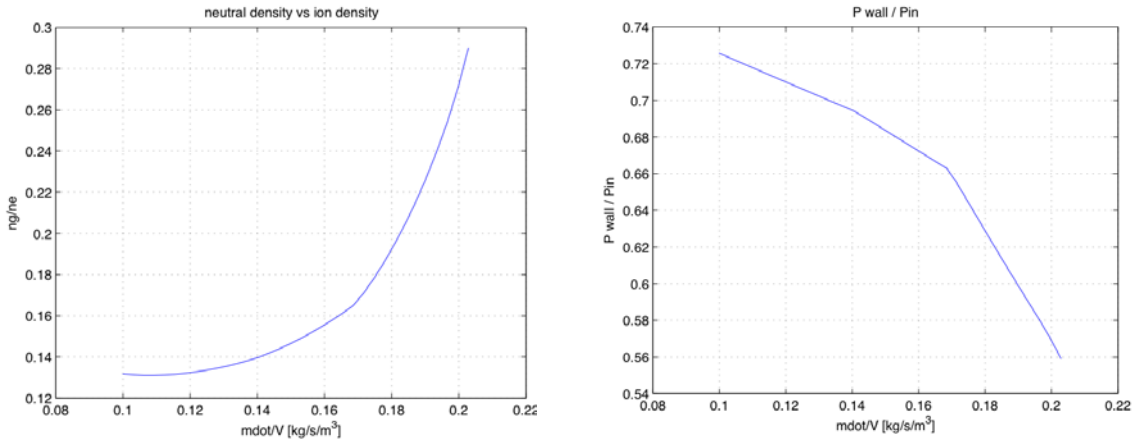

Figure 6 ration between ion density and residual neutral density , and ration between power loss at the wall and applied external power versus mass flow rate normalized on the source volume, moreover

As shown in Figure 6 increasing the mass flow rate correspond to a reduction on ionization fraction, represented by the ratio between residual neutral density and electron density, moreover less input power get lost at the wall.

After the preliminary sizing of the thruster it has been also estimated the power to be dissipated by the radiator, assessed conservatively as total power minus jet power. Its value has been estimated to be 1100 W.

IV. Thermo-Mechanical Preliminary Design

In the following Figure 7 it is reported a sketch of the thruster configuration hereafter considered. The dielectric cylindrical wall having external diameter of 35 mm and being 87 mm in length is attached to an interface plate that it will be connected to the spacecraft. The helicon antenna is wrapped around the dielectric quarts tube. Moreover a metallic shell is placed around the antenna in order to support the insulating material and finally the superconducting coils with its support/cooling element.

The superconducting coil has been considered in order to save mass and volume[44]. The main superconductors features from which enormous benefits on board spacecraft may result are:

- ability to carry high current densities which leads to substantial coil weight and dimensions reduction;
- at critical temperature electrical resistivity decreases to an immeasurable value: it means that ohmic heating of the magnet coil drops to zero, i.e., on electrical power must be wasted and current flow, starting in the wire, keeps the same intensity indefinitely.

Superconductivity at low temperature requires liquid helium at 4.2 K to produce very high current densities: the thermal analysis shows that high temperature superconductors are preferable because these can support lower current densities but with a higher critical superconductivity temperature (>77 K), easier to maintain during the whole mission. The material chosen is a BSCCO (Bismuth Strontium Calcium Copper Oxide) high temperature superconductor. Option of using permanent magnet has also been considered, however, the generated magnetic field are normally strongly non-uniform, with reversal regions and null points (cusps)[45]. Such the strong non-uniformity can impede the wave propagation and plasma flow, and thus eliminate the effects of enhanced plasma production and potential drop formation. Thus, accurate numerical model and experimental investigation need to be carried out prior to proceed with a detailed thruster design based on this technology. In this research work attention has been focused only on superconductor option thanks to the lower uncertainty on design associated to this solution.

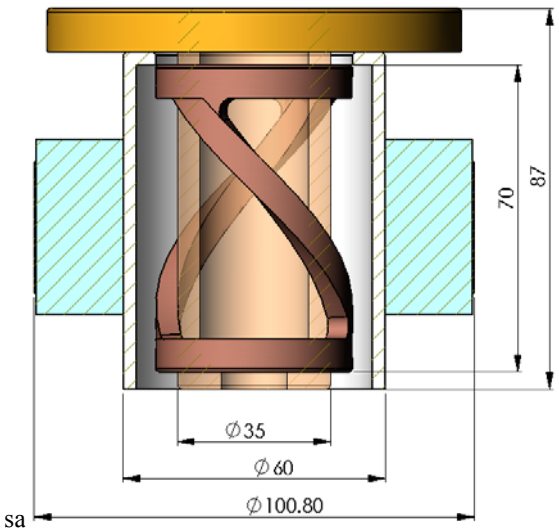

Figure 7 Schematic section view of plasma motor

A. Thermal analysis

A sensitivity study has been performed on a simplified thermal model of the thruster.
In the Figure 8 is reported a schematic view of the plasma thruster considered on the steady state thermal analysis. The model has been implemented using ESARAD & ESATAN software.
The parameter considered for the sensitivity study has been: (i) boundary support interface temperature, (ii) boundary radiative external environment temperature, (iii) support interface material conductivity (S/C interface temperature), (iv) the plasma power. The temperature reached from the different part of thruster and the expected thermal fluxes for each case has been evaluated. The material considered for the main parts are: fused quartz for antenna support, aluminum alloy (thermal conductivity 170 W/(m·K)) or titanium alloy (thermal conductivity 7 W/(m·K)) for the support.

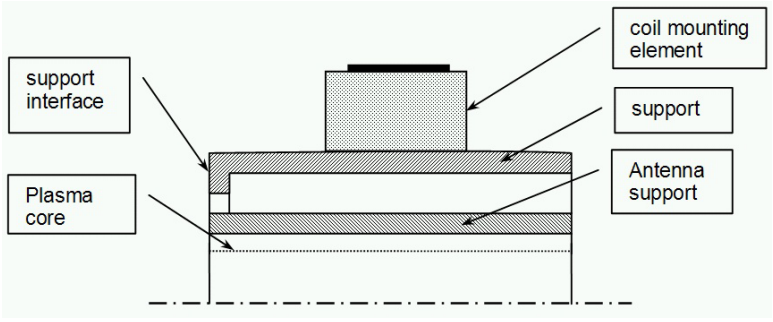

Figure 8 Schematic section view of plasma motor

In the Figure 9 has been reported the mean temperature obtained for different temperature of boundary support interface (at the S/C interface) when the support is realized with aluminum alloy; considering that for these alloy the max temperature in service can be reach 250÷280 °C a reasonable upper limit for the boundary temperature interface could be 50 °C. The temperature evaluated for the antenna support represent a worst case estimation, in fact in the model this part has been considered conductively thermal decoupled from the support interface, in any case the temperature reached is compatible with the max continuous temperature for the fused quartz, 1000 °C; further detailed model that implement also the low conductive link for the antenna support with the support interface will allow to reduce a little bit its mean temperature. The results in any case highlight that the thermal flux generated by the plasma in this configuration should be removed from the support interface for the 75% and only a 25% is exchanged radiatively with the external environment. This is due to the reduced dimensions of the system and the relatively low temperature of support part.
The thermal flux at support boundary interface could be moved at the spacecraft radiator with dedicate heat pipes. Assuming a spacecraft radiator with the dimension of 1350x1350 [mm] temperature of 40 °C with a emissivity ε=0.8 the dissipated thermal flux is about 800 W. The radiator interface could be reduced increasing the S/C radiator temperature.

Boundary support interface temperature [°C]	Support Mean temperature [°C]	Antenna Support Mean temperature [°C]
-20	185	968
-10	194	968
0	204	968
10	213	969
20	222	969
80	277	972
150	340	976

Radiative environment temperature = -10 °C
Conductive thermal flux at support interface = ~ 530 W
Radiative thermal flux at support interface = ~ 220 W
Radiative thermal flux at external environment = ~ 250 W

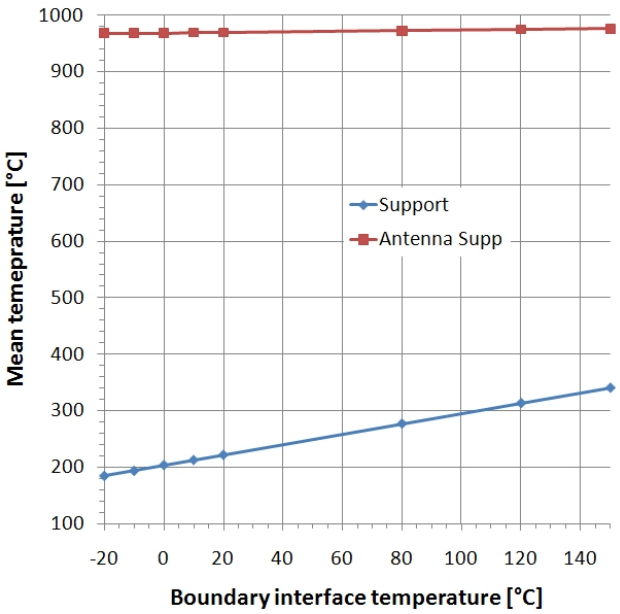

Figure 9 Effect of S/C interface temperature ; support realized with thermally conductive material (eg. Aluminum alloy)

Analysis has been also done using: (i) titanium alloy (Ti 6Al 4V) for the support, (ii) support boundary temperature of 20°C and a (iii) radiative environment temperature of -10°C. Results show that the exchanged flux with the support boundary interface is reduced (thermal flux ~400 W) while the radiative flux exchanged with the environment is increased (~600 W). This lead to higher temperature of different parts of the system: the support reach about 750 °C and the antenna support overcome the 1050 °C. The high temperature of the support requires a more effort to thermally decouple the coil element from the support, but in any case the S/C radiator area could be halved. Further analysis will be performed in order to asses a trade off for the required resources at system level.

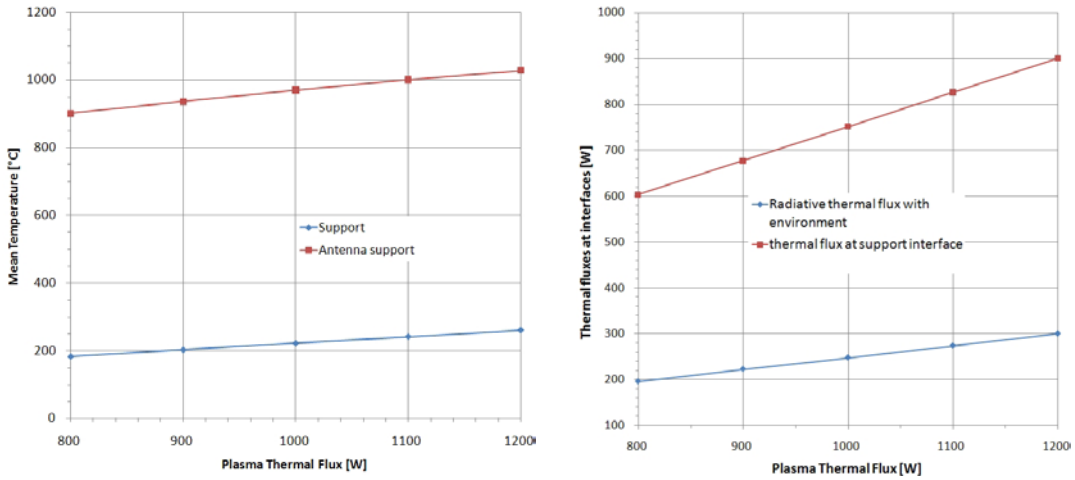

Figure 10 On the left support and antenna support temperature versus thermal plasma dissipate power, on the right thermal fluxes at interfaces; (support boundary temperature = 20 °C, radiative environment = -10 °C)

Figure 10 show the temperature of support and antenna support and the thermal fluxes at interfaces with reference to the configuration characterized by: (i) aluminum alloy support, (ii) support boundary temperature of 20°C, (iii) a radiative environment temperature of -10°C, and (iv) a dissipated thermal power from the plasma between 800÷1200 [W]. An increase of 100 W on thermal plasma flux means a mean increase on support temperature of 20 °C and of 30 °C on antenna support. The ratio of thermal fluxes at interfaces versus the plasma thermal flux not change significantly in the range considered.

Further analysis on more detailed model will be performed in order to evaluate with more detail the antenna support temperature and the antenna temperature versus its electrical resistivity considering different mounting configuration.

The use of superconductor tapes for the generation of the required magnetic field makes it possible to save mass, volume and power. On the other side, the thermal control of superconductor materials is a critical issue because they require very low operating temperatures. The material chosen is BSCCO (Bismuth Strontium Calcium Copper Oxide) which is a high temperature superconductor with a critical temperature of 105 K. Therefore the operating temperature is set to 40 K, accounting for a safety margin.

In the previous simulation, considering the coil mounting element realized with silica aerogel to thermally decouple the parts from the support, the expected thermal flux that should be removed from coil at temperature of 40 K is about 8.5 W with aluminum support or 18 W with titanium support. To remove this thermal flux there are some possible solutions with different system impact and that should be evaluated after a trade off process.

- The first possibility (in the case of aluminum support) should be to remove the thermal flux from low temperature coil with a dedicate crycooler.
- The second possibility is to remove a fraction of this flux with a dedicate radiator in order to have a lower part of flux that should be removed from the coil at low temperature with a minor resources demanding crycooler.

For example, considering the case of aluminum support, if a dedicate radiator is foreseen to have an intermediate temperature of -20°C the flux at the radiator should be about 4.8 W (at coil part remains about 3.7 W to be removed) and assuming a radiator temperature of -30 °C with a emissivity ε =0.8 its minimal dimensions should be 190x190 mm. Figure 11 shows a possible architecture capable of reduce thermal flux at coli part.

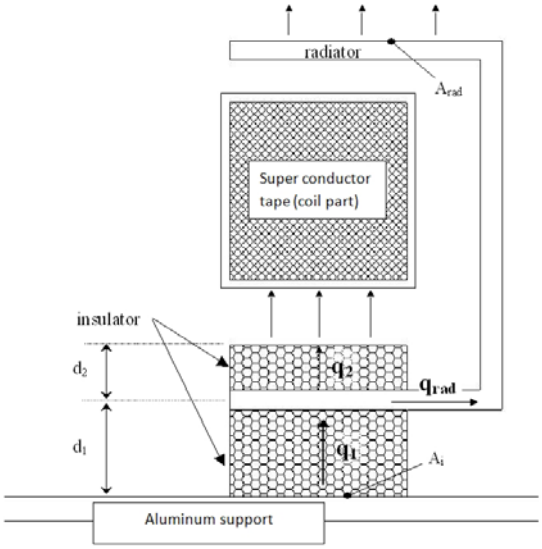

Figure 11 Possible architecture to reduce the thermal flux at coil part

B. Mechanical analysis

For the previous thruster scheme a Finite Model Element has been developed with MSC-Nastran for Windows software to evaluate the eingenfrequencies of the system and the stress level in the main components at quasi static loads. The model is realized with plate elements, the materials considered for the support is aluminum alloy (7075-T6) while fused quartz is used for the antenna support. The mass of helicon has been locally distributed on the antenna support. The mass of coil and coil mounting element has been locally distributed on support part. For the connection between quartz and interface plate a disk of inconel or invar are assumed for the dynamic and static evaluation

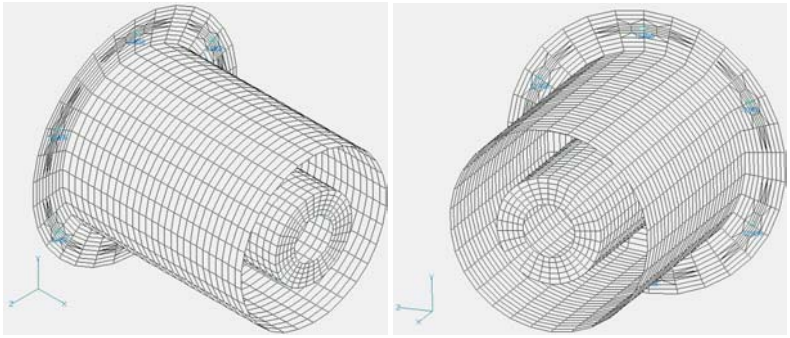

Figure 12 Finite element model, isometric view

The model show in Figure 12 is composed from 2569 elements and 2526 nodes. Two type of analysis has been carried out, the normal modes and the static one. The first evaluation is aimed to verify that the eigenfrequency of the structure is higher of 150 Hz (value referred to the payload mounted on a S/C) while the second analysis considers a quasi static load applied spherically (in case of Arianne 5 launcher at the S/C primary interfaces for a payload with a mass lower of 1 kg the quasi static acceleration is 700 m/s^2).

Some results are reported in the following images, the first eigenfrequency is 885 Hz, with flexional mode shape, the max displacement at the quasi static loads is 0.06 mm while the max stress (Von Mises criteria) for the support part is about 25 MPa and for the antenna support component is 6 MPa.

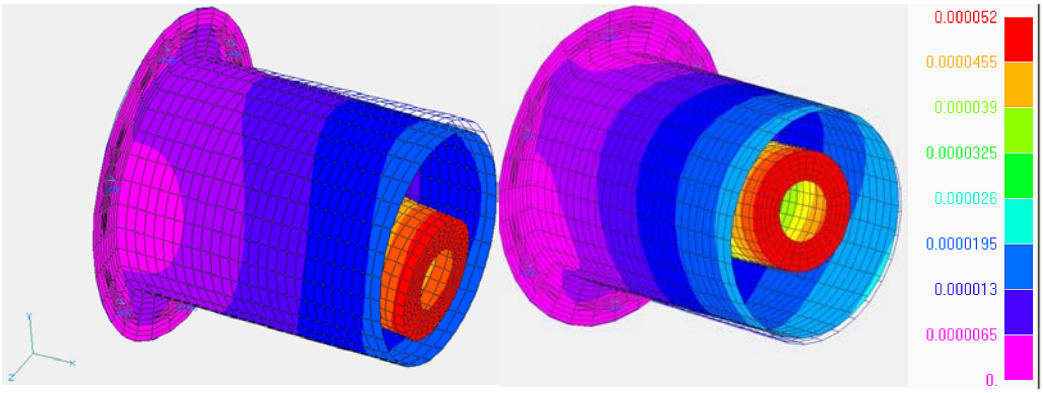

Figure 13 on the left the first eigen-mode of the system, on the right the displacement (in meter) at quasi static load acting spherically along the positive axis directions.

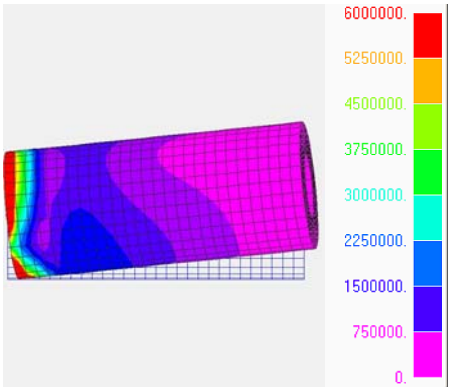

Figure 14 Max stress evaluated with Von Mises criteria for the antenna support component considering the quasi static loads, (Pa).

In all cases the results fulfill the requirements for the structural feasibility study, additional detailed thermo elastic analysis should be carried out to refine the interface between support and antenna support to accommodate the different CTE materials and reduce the local stress concentration.

Part	Mass [g]
Support	120
Antenna support	75
Coil mounting element	90
Helicon	125
Total	**410**

V. Conclusion

A preliminary design of a medium power helicon plasma thruster has been conducted through: (i) analysis and optimization of the plasma section, (ii) preliminary thermo-mechanical analysis and design. The magnetic section has been sized considering superconductor, which have a strong impact at system level. A more efficient solution is probably to use permanent magnet, however, due to irregularities in the magnetic field-space-configuration, this solution need to be carefully analyzed with 3-D code (non available in the present study) and dedicated test campaign. Preliminary analysis showed that the structural part of the thruster can be kept below 1kg. To this mass budget need to be added the mass of RF power unit, magnetic field control unit.

References

[1]Pavarin D, "Diagnostic and optimization procedures for gas and plasma propulsion system", PhD thesis, University of Padova, 2001.

[2]Goulding RH, Pavarin D, Angrilli F, Barber GC, Carter MD, Maggiora R, Sparks DO, "Helicon plasma source configuration analysis by means of density measurements" ICEAA, Torino, Italy, 1999.

[3]Rocca S, "Design and modeling of an experiment for the performance evaluation of a variable specific impulse magnetoplasmadynamic thruster", PhD thesis in Mechanical Measurements for Engineering, University of Padova, 2005.

[4]Goulding RH, Baity FW, Barber GC, Carter MD, CHANG Díaz FR, Pavarin D, Sparks DO, Squire JP, "Helicon plasma source optimization studies for VASIMR", APS 99 Meeting.

[5]Suwon C, "A self consistent global model of neutral gas depletion in pulsed helicon plasmas", Physics of plasmas, vol 6, Jan 1996, pp. 359-365.

[6]Gilland J, "Neutral Pumping in a Helicon Discharge", Plasma Sources Sci Tec n 7, 1998, pp 416-422.

[7]Zorat R, "Global model of a radio frequency H2 plasma in DENISE", Plasma Sources Sci Tech 9 (2000) 161-168.

[8]Chung TH, "Global model and scaling laws for inductively coupled oxygen discharge plasmas" J. Appl. Phys vol 86, n. 7 Oct, 1999.

[9]Lee C, J. Electrochem. Soc vol 14-1, N°6, June 1994.

[10]Cheetham AD, "Characterization and modelling of a helicon plasma source" J. Vac. Sci. Tech. A 16(5) Sep-Oct 1998.

[11]Lieberman MA, "Global Model of pulse-power-modulate high-density, low-pressure discharges" Plasma Sources Sci. Tech. 5, (1996) 145-158.

[12]Lee C. "Global Model of Plasma Chemistry in a High Density Oxygen Discharge" J.Electrochem.Soc, Vol.141, No. 6, June 1994.

[13]Ashida S. "Spatially averaged (Global) model of time Modulated High Density Chlorine Plasmas, J.Appl.Phys. Vol. 36, (1997), pp. 854-861.

[14]Ashida S. "Spatially averaged (global) model of time modulated high density argon plasmas", J.Vac.Sci.Tech. A 13(5), Sep/Oct 1995.

[15]Meyyappan, M., "A spatially-averaged model for high density discharges", Vacuum, Vol 47, N.3, 215-220, 1996.

[16]Gordies, B. "Self-consistent kinetic model of low-pressure N2-H2 flowing discharges I-II", Plasma sources Sci. Tech 7(1998), 378-388.

[17]Lee, C. , "Global model of Ar, O2, Cl2, and Ar/O2 high-high density plasma discharges", J.Vac.Sci.Tech. A 13(2) Mar/Apr 1995.

[18]Nakano, T. , "Ion and neutral temperature in electron cyclotron resonance plasma reactors", Appl.Phys.Lett 58(5) 1991, pp. 458-460.

[19]Hopwood , J. ,"Nuetral gas temperature in a multipolar electron cyclotron resonance plasmas", Appl. Phys. lett 58 (22), 3 Jun,1991.

[20]Milora, S. L. , "Quickgun: an algorithm for estimating the performance of two-stage light gas guns" ORNL/TM-11561 report.

[21]Mitchner, M. , Partially Ionize Gases, A.Willy, 1973, New York.

[22]McDaniel, E. W. , Collision phenomena in ionized gases, John Willey & sons New York 1964.

[23]Janev, R. K. , Elementary processing hydrogen helium plasmas, Springer-Verlag, 1987.

[24]Barnet, C. F. "Collision of H,H2,He and Li atoms and ions with atoms and molecules". ORNL

[25]Godyak V A 1986 S.

[26]Mozetic, M. "Atomic hydrogen density along continuously pumped glass tube", Vacuum, vol.5, n°3-4 pp. 319-322, 1998.

[27]Tynan, G. R. "Neutral depletion and transport mechanism in large-area high density plasma sources", Journal of applied physics vol 86, n°10, Nov 1999.

[28]Lieberman, M.A, "Principles of Plasma Discharges and Material Processing", New York Wiley, 1994.

[29]Lee, C. Journal of Electroch. Soc, vol 141, n°6 Jun, 1994.

[30]Dushmann, Scientific foundation of vacuum technique, John Willey & Sons inc. NY 1964.

[31]Holland, L. , Vacuum Manu, l, F.N. Spon, London

[32]Chapman, The mathematical theory of non uniform gas, Cambridge At the University Press 1970.

[33]Panevsky, M. I., “Characterization of the Resonant Electromagnetic Mode in Helicon Discharges” PhD Thesis, University of Texas at Austin, 2003.
[34]Verboncoeur, J.P., Langdon, A.B. , and Gladd, N.T. , "An Object -Oriented Electromagnetic PIC Code", Comp. Phys. Comm., 87, May11, 1995, pp. 199-211.
[35]Birdsall C., Langdon A. ”Plasma Physics via computer simulation” Iop, Bristol, 1991
[36]Raadu, A. ”Particle Acceleration Mechanisms in Space Plasmas”, Phys. Chem. Earth (C), Vol. 26, No. 1-3, pp.55-59, 2001
[37]Raadu, A. ”The physics of double layers and their role in astrophysics”, Physics Reports 178, No2, 1989, pp25-97.
[38]Perkins and Sun, Y.C. ”Double Layers without current” Phys. Rev. Lett. 46, 115 (1981)
[39]Chan, M.H. Cho, N. Hershkowitz, T. Intrator, ” Experimental observation of slow ion acoustic Double Layers” Phys. Rev. Lett. 57, 3050 (1986)
[40]Charles,C., Boswell, R.W. , ”Laboratory evidence of a supersonic ion beam generated by a current-free ”helicon” doublelayer”. Phys. Plasmas 11, 1706-1714 (2004).
[41]Charles,C., ”Hydrogen ion beam generated by a current-free double- layer in a helicon plasma”. Applied Physics Letters 84, 332-334 (2004)
[42]Charles,C. and Boswell, R.W. , ”Current-free double-layer formation in a high -density helicon discharge”. Applied Physics Letters 82, 1356 -1358 (2003).
[43]Manente, M. , Carlsson, J. , Musso, I. , Bramanti, C. , Pavarin, D., and Angrilli, F. “Numerical simulation of the Helicon Double Layer Thruster Concept” 8 - 11 Jul 2007 43rd AIAA/ASME/SAE/ASEE Joint Propulsion Conference
[44]Bruno,C., Giucci,S. “Cryogenic technology to improve electric thrusters” Acta astronautica Vol. 51, No. 12, pp. 855-863, 2002
[45]Shamrai, K. P., Virko, Y. V. , Virko, V. F., Yakimenko, A. I. , “Compact Helicon Plasma Source with Permanent Magnets for Electric Propulsion Application“ 42nd AIAA/ASME/SAE/ASEE Joint Propulsion Conference & Exhibit 9 - 12 July 2006, Sacramento, California